

News on Compton Scattering $\gamma X \rightarrow \gamma X$ in Chiral EFT

Harald W. Griebhammer^{1,a}, Judith A. McGovern², and Daniel R. Phillips³

¹ *Institute for Nuclear Studies, Dept. of Physics, George Washington University, Washington DC 20052, USA*

² *School of Physics and Astronomy, The University of Manchester, Manchester M13 9PL, UK*

³ *Dept. of Physics and Astronomy, Inst. of Nucl. and Part. Physics, Ohio University, Athens OH 45701, USA*

Abstract. We review theoretical progress and prospects to understand the nucleon's static dipole polarisabilities from Compton scattering on few-nucleon targets, including new values; see Refs. [1–5] for details and a more thorough bibliography.

Why Compton Scattering? Since the electromagnetic field of a real photon induces radiation multipoles by displacing charged constituents and currents, the energy- and angle-dependence of the emitted radiation elucidates the distribution, symmetries and dynamics of the charges and currents which constitute the low-energy degrees of freedom inside the nucleon and nucleus; see e.g. a recent review [1]. *Energy-dependent polarisabilities* parametrise the stiffness of the nucleon N (spin $\frac{\sigma}{2}$) against transitions $Xl \rightarrow Yl'$ of given photon multipolarity at fixed frequency ω ($l' = l \pm \{0; 1\}$; $X, Y = E, M$; $T_{ij} = \frac{1}{2}(\partial_i T_j + \partial_j T_i)$; $T = E, B$). Up to 500 MeV in photon energy, the relevant terms are:

$$\begin{aligned} \mathcal{L}_{\text{pol}} = & 2\pi N^\dagger [\alpha_{E1}(\omega) \vec{E}^2 + \beta_{M1}(\omega) \vec{B}^2 + \gamma_{E1E1}(\omega) \vec{\sigma} \cdot (\vec{E} \times \vec{E}) + \gamma_{M1M1}(\omega) \vec{\sigma} \cdot (\vec{B} \times \vec{B}) \\ & - 2\gamma_{M1E2}(\omega) \sigma^i B^j E_{ij} + 2\gamma_{E1M2}(\omega) \sigma^i E^j B_{ij} + \dots \text{ (photon multipoles beyond dipole)}] N \quad (1) \end{aligned}$$

Two scalar polarisabilities $\alpha_{E1}(\omega)/\beta_{M1}(\omega)$ encode electric/magnetic dipole transitions; 4 spin-polarisabilities $\gamma_{E1E1}(\omega)$, $\gamma_{M1M1}(\omega)$, $\gamma_{E1M2}(\omega)$ and $\gamma_{M1E2}(\omega)$ the response of the nucleon's spin-structure. Intuitively interpreted, the electromagnetic field associated with the spin degrees causes bi-refringence in the nucleon (Faraday-effect).

Polarisabilities test our understanding of the subtle interplay between electromagnetic and strong interactions and enter in theoretical determinations of the proton-neutron mass difference, and in the two-photon-exchange contribution to the Lamb shift in muonic hydrogen; see e.g. the introduction of [5]. Finally, nuclear targets provide an opportunity to study not only neutron polarisabilities, but indirectly also the nuclear force, since the photons couple to the charged pion-exchange currents in the nucleus. The values $\alpha_{E1}(\omega = 0)$ etc. are often called “the (static) polarisabilities”; they compress the richness of information extrapolated from data in a wide range of energies between about 70 MeV and the Δ resonance region into just a few numbers. In the canonical 10^{-4} fm^3 , Chiral Effective Field Theory (χ EFT, see below) gives (Fig. 1 and [2, 4]):

$$\begin{aligned} \alpha_{E1}^{(p)} &= 10.65 \pm 0.35_{\text{stat}} \pm 0.2_{\text{Baldin}} \pm 0.3_{\text{th}} \quad , \quad \beta_{M1}^{(p)} = 3.15 \mp 0.35_{\text{stat}} \pm 0.2_{\text{Baldin}} \mp 0.3_{\text{th}} \\ \alpha_{E1}^{(n)} &= 11.55 \pm 1.25_{\text{stat}} \pm 0.2_{\text{Baldin}} \pm 0.8_{\text{th}} \quad , \quad \beta_{M1}^{(n)} = 3.65 \mp 1.25_{\text{stat}} \pm 0.2_{\text{Baldin}} \mp 0.8_{\text{th}} \quad (2) \end{aligned}$$

^ae-mail: hgrie@gwu.edu; presenter.

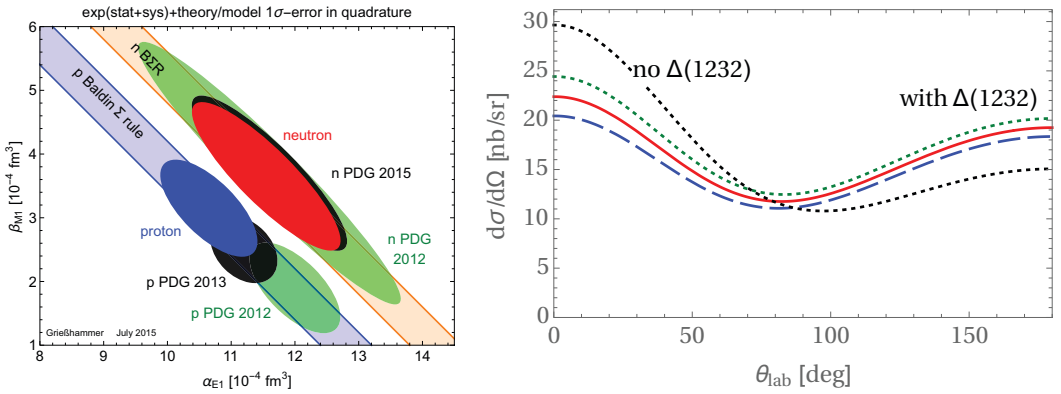


Figure 1. *Left:* Static scalar polarisabilities in our fits (red: proton; blue: neutron); old (green) and new (black) PDG values. 1σ errors, with statistic, systematic and theory error added in quadrature. *Right:* ^3He Compton scattering at 120 MeV with $\Delta(1232)$ (red solid), and without (black dotted); blue dashed/green dotted: $\alpha_{E1}^{(n)} \pm 2$.

We also predicted the spin values [2, 5], prior to the pioneering MAMI results [6] (in 10^{-4} fm^4):

	γ_{E1E1}	γ_{M1M1}	γ_{E1M2}	γ_{M1E2}	
$\chi\text{EFT neutron}$	$-4.0 \pm 1.9_{\text{th}}$	$1.3 \pm 0.5_{\text{stat}} \pm 0.5_{\text{th}}$	$-0.1 \pm 0.6_{\text{th}}$	$2.4 \pm 0.5_{\text{th}}$	(3)
$\chi\text{EFT proton}$	$-1.1 \pm 1.9_{\text{th}}$	$2.2 \pm 0.5_{\text{stat}} \pm 0.6_{\text{th}}$	$-0.4 \pm 0.6_{\text{th}}$	$1.9 \pm 0.5_{\text{th}}$	
proton MAMI 2014	-3.5 ± 1.2	3.2 ± 0.9	-0.7 ± 1.2	2.0 ± 0.3	

M. Ahmed and L. Myers reported on the concerted ongoing and planned efforts at HIγS [7], MAX-Lab [4, 8], and MAMI [9]. Interpreting such data requires of course commensurate theory support; cf. the open letter by theorists from a variety of backgrounds Ref. [10]. One must carefully evaluate data-consistency for hidden systematic errors; subtract binding effects in few-nucleon systems; extract the polarisabilities; identify their underlying mechanisms and relate them to QCD – and all that with reproducible theoretical uncertainties and minimal theoretical bias.

Indeed, χEFT , the low-energy theory of QCD and extension of Chiral Perturbation Theory to few-nucleon systems, has been quite successful in proton and few-nucleon Compton scattering. With $\delta \equiv \frac{\Delta_M}{\Lambda} \approx \left(\frac{m_\pi}{\Lambda}\right)^{1/2} < 1$ [11], we recently derived single-nucleon Compton amplitudes from zero energy to about 400 MeV. For $\omega \lesssim m_\pi$, they contain all contributions at $\mathcal{O}(e^2\delta^4)$ (N^4LO , accuracy $\delta^5 \lesssim 2\%$), and for $\omega \sim \Delta_M$ all at $\mathcal{O}(e^2\delta^0)$ (NLO, accuracy $\delta^2 \lesssim 20\%$) [1, 2]. A reproducible and systematically improvable *a priori* estimate of the theoretical accuracies of observables, like in eqs. (2) and (3) or Fig. 5, is essential to uniquely disentangle chiral dynamics from data; see Ref. [5] and Refs. therein.

Figure 2 lists examples of the 3 classes of contributions in few-nucleon systems. Charged exchange currents and rescattering often dominate over the nucleonic structure contributions. Compton photons therefore also provide direct, non-trivial benchmarks how accurately the chiral expansion accounts order-by-order for nuclear binding and its mesonic contributions. For the deuteron, our results are complete at $\mathcal{O}(e^2\delta^3)$ from the Thomson limit up to about 120 MeV, including the $\Delta(1232)$ [1].

In the preceding talk, L. Myers eloquently described the difficulties and successes of adding 22 deuteron points at MAXlab [4, 8]. This first new data in over a decade effectively doubled the deuteron's world dataset. Our analysis shows that is well consistent with and within the world dataset ($\chi^2 = 45.2$ for 44 degrees of freedom), and with the Baldin sum rule. These data alone slashed the statistical error by 30%. Just to illustrate the data quality, Figure 3 shows that the χ^2 distribution of the new world dataset agrees quite well with the analytic expectation.

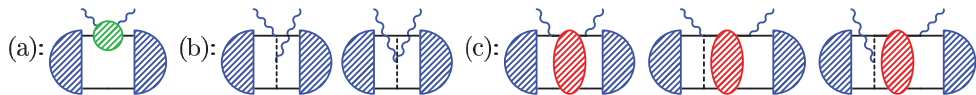


Figure 2. Contributions to deuteron Compton scattering. Ellipse: NN S -matrix:(a): single-nucleon; (b) photon coupling to charged exchange currents which bind the nucleus as dictated by chiral symmetry; (c) rescattering between emission and absorption restores the low-energy Thomson limit and guarantees current conservation.

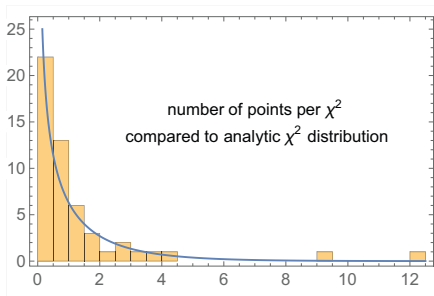


Figure 3. Histogram of the number of deuteron Compton data with a given χ^2 , overlaid with the predictions of an ideal, statistically consistent set. The two data with $\chi^2 \geq 9$ are pruned by statistical-likelihood criteria; including them does not have a significant impact on the neutron values. We add point-to-point and angle-dependent systematic errors in quadrature to the statistical error, and subsume overall systematic errors into a floating normalisation. The norm of each dataset floats by $\leq 5\%$ and within the respective quoted normalisation errors of the data.

The future lies in un-, single- and double-polarised experiments of high accuracy and theoretical analyses with reproducible systematic uncertainties. To understand the subtle differences of the pion clouds around the proton and neutron induced by explicit chiral symmetry breaking in QCD, we need the neutron polarisabilities with uncertainties comparable to those of the proton – eq. (2) shows that this is mostly an issue of better data. Therefore, MAMI, MAXlab and HIγS aim for deuteron data with statistical and systematic uncertainties of better than 5%, and plan extensions to ^3He . In general, heavier nuclei are experimentally better to handle and provide count rates which scale at least linearly with the target charge when photons scatter incoherently from the protons, i.e. for $\omega \gtrsim 100$ MeV. But a theoretical description of their energy levels with adequate accuracy is involved. For the proton, amplitudes on the $\leq 2\%$ -level are available; for deuteron and ^3He , we now extend descriptions with similar accuracies into the Delta resonance region. Around ^3He - ^4He - ^6Li may well be the “sweet-spot” between needs and wants of theorists and experimentalists. Figure 1 shows that not including the $\Delta(1232)$ can lead to false signals in high-accuracy extractions of neutron polarisabilities [12].

Since the 8 spin-polarisabilities are a top priority of experiment and theory alike, we performed a series of sensitivity studies; see Fig. 4 and summary in [1, Sec. 6.1]. Recently, the deuteron cross section and asymmetry with arbitrary photon and target polarisations has for example been parametrised via 18 independent observables [3]. Particularly attractive are some asymmetries which are sensitive to only 1 or 2 polarisabilities. For spin polarisabilities with an error of $\pm 2 \times 10^{-4} \text{ fm}^4$, asymmetries should be measured with an accuracy of $\gtrsim 10^{-2}$, with differential cross sections of a dozen nb/sr at 100 MeV or a few dozen nb/sr at 250 MeV. Relative to single-nucleon Compton scattering, interference with the deuteron’s D wave and pion-exchange current increases the sensitivity to the “mixed” spin polarisabilities γ_{E1M2} and γ_{M1E2} . A *Mathematica* file for $\omega < 120$ MeV is available from hgrie@gwu.edu (see screen-shot in Fig. 4), and is finalised for the proton and ^3He .

Finally, χEFT connects data with emerging lattice-QCD simulations by reliable extrapolations from numerically less costly, heavier pion masses within the χEFT regime to the physical point and circumvents a direct lattice simulation of Compton scattering – that would be highly nontrivial. The lattice, in turn, tests to which extent χEFT adequately captures the m_π -dependence of the low-energy dynamics, and may predict short-distance (fit) parameters from QCD. W. Detmold’s plenary showed intriguing lattice results for the proton’s and neutron’s β_{M1} at $m_\pi = 806$ MeV; see Fig. 5 and Ref. [5].

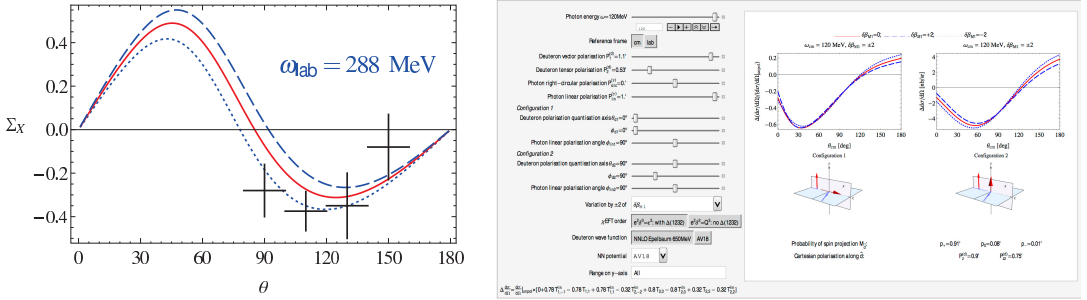


Figure 4. Left: χ EFT prediction and MAMI data [6] for the double-polarisation observable Σ_{2x} on the proton. Solid: $\gamma_{E1E1} = -1.1$ (predicted); dashed/dotted: theory uncertainty from eq. (3) and Ref. [5]. Right: Mathematica notebook screenshot for deuteron Compton scattering with arbitrary polarisations [3].

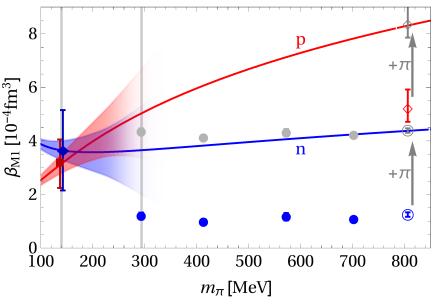


Figure 5. Comparison of our χ EFT predictions to lattice simulations of β_{M1} : \bullet (neutron) Hall et al.; \diamond (proton) and \circ (neutron) NPLQCD. Gray “ghost points” found by shifting all lattice results by $+\pi \times 10^{-4} \text{ fm}^3$ [sic!]. The difference $\beta_{M1}^{(p)} - \beta_{M1}^{(n)}$ is nearly identical to the chiral result even well beyond the range in which χ EFT should be applicable. This suggests that the experimental finding $\beta_{M1}^{(p)} \approx \beta_{M1}^{(n)}$ is something of a coincidence. The agreement with simulations for α_{E1} is even better [5]. Corridors: theoretical uncertainties in the regime where χ EFT can be expected to converge [5].

Acknowledgements

HWG cordially thanks the organisers for a stimulating atmosphere and incessant promotion of Chicago’s highlights of popular comics culture. This work was supported in part by UK Science and Technology Facilities Council grants ST/J000159/1 and ST/L005794/1 (JMcG), by the US Department of Energy under contracts DE-FG02-93ER-40756 (DRP) and DE-FG02-95ER-40907 (HWG), and by the Dean’s Research Chair programme of the Columbian College of Arts and Sciences of The George Washington University (HWG).

References

[1] H.W. Griebhammer, J.A. McGovern, D.R. Phillips, G. Feldman, Prog.Part.Nucl.Phys.**67**,841(2012).
 [2] J. A. McGovern, D. R. Phillips and H. W. Griebhammer, Eur. Phys. J. A **49** 12 (2013).
 [3] H. W. Griebhammer, Eur. Phys. J. A **49** 100 (2013).
 [4] L. S. Myers *et al.* [COMPTON@MAX-lab Collaboration], Phys. Rev. Lett. **113**, 262506 (2014).
 [5] H. W. Griebhammer, J. A. McGovern and D. R. Phillips, arXiv:1511.01952.
 [6] P. P. Martel *et al.* [A2 Collaboration], Phys. Rev. Lett. **114**, 112501 (2015).
 [7] H. R. Weller *et al.*, Prog. Part. Nucl. Phys. **62** 257 (2009).
 [8] L. Myers *et al.*, Phys. Rev.**C92** 025203 (2015).
 [9] G. M. Huber and C. Collicott, arXiv:1508.07919 [nucl-ex].
 [10] H. W. Griebhammer, A. I. L’vov, J. A. McGovern, V. Pascalutsa, B. Pasquini and D. R. Phillips, arXiv:1409.1512 [nucl-th].
 [11] V. Pascalutsa and D. R. Phillips, Phys. Rev. C **67**, 055202 (2003).
 [12] H. W. Griebhammer, J. A. McGovern, D. R. Phillips, D. Shukla and B. Strandberg, forthcoming.